# Root electrotropism in *Arabidopsis* does not depend on auxin distribution, requires cytokinin and follows a power-law response curve

Nicholas Oliver[1,2,§], Maddalena Salvalaio[1,§], Deniz Tiknaz[1,3], Maximillian Schwarze[1,4], Nicolas Kral[1,5], Soo-Jeong Kim[1], Giovanni Sena[1,*]

[§] These authors contributed equally to this work.

[1] Department of Life Sciences, Imperial College London, UK

[2] Present address: Department of Physics, Freie Universität Berlin, Germany

[3] Present address: National Heart & Lung Institute, Imperial College London, UK

[4] Present address: School of Biosciences, University of Birmingham, UK

[5] Present address: Phytoform Labs Ltd., Lawes Open Innovation Hub, Harpenden, UK

*Corresponding author: Giovanni Sena

**Email:** g.sena@imperial.ac.uk

**Abstract**

An efficient foraging strategy for plant roots relies on the ability to sense multiple physical and chemical cues in soil and to reorient growth accordingly (tropism). Root tropisms range from sensing gravity (gravitropism), light (phototropism), water (hydrotropism), touch (thigmotropism) and more. Electrotropism, also known as galvanotropism, is the phenomenon of aligning growth with external electric fields and currents. Although observed in a few species since the end of the 19th century, the molecular and physical mechanism of root electrotropism remains elusive, limiting the comparison to more defined sensing pathways in plants.

Here we provide a first quantitative and molecular characterisation of root electrotropism in the model system *Arabidopsis thaliana,* showing that it does not depend on an asymmetric distribution of the plant hormone auxin but that, instead, it requires the biosynthesis of a second hormone, cytokinin. We also show that the dose-response kinetics of root electrotropism follows a power law analogous to the one observed in common animal physiological reactions, suggesting universal properties.

A full molecular and quantitative characterisation of root electrotropism would represent a step forward towards a better understanding of signal integration in plants, and an independent outgroup for comparative analysis of electroreception in animals and fungi.

## Introduction

Plant roots navigate the complex soil environment in search of water and nutrients, through various sensing mechanisms reorienting their growth towards or away from signal sources (tropism) (Muthert et al., 2020). For example, hydrotropism redirects growth towards high moisture (Miyazawa and

Takahashi, 2019), (negative) phototropism redirects away from light sources (Kutschera and Briggs, 2012), and gravitropism induces growth downwards, following the gravity vector (Su et al., 2017). The integration of overlapping and frequently contradicting molecular and physical signals is as critical for plant roots as it is for other soil organisms (Iino, 2006)

Although many molecular aspects of a few root tropisms have been understood (Muthert et al., 2020), several key sensing mechanisms remain elusive. One of these is the capacity of plant roots to sense electric fields (electrotropism or galvanotropism) (Navez, 1927). The reception of electric fields (electroreception) has been observed in vertebrates (Crampton, 2019) and invertebrates(Clarke et al., 2013), including common model systems such as *C. elegans* (Sukul and Croll, 1978) and *Dyctostylium* (Shanley et al., 2006), as well as in fungi (McGillivray and Gow, 1986). Interestingly, electric sensing structures have been identified only in a few aquatic animal species (Peters et al., 2007) and more recently in bumble-bees (Sutton et al., 2016).

First recorded in 1882 (Elfving, 1882) and rediscovered at the start of the 20$^{th}$ century (Ewart and Bayliss, 1905), root electrotropism has been studied sporadically in maize (*Zea mays*), peas (*Pisum sativum*) and bean (*Vigna mungo*) but with contradicting results (Ishikawa and Evans, 1990; Stenz and Weisenseel, 1993; Wolverton et al., 2000). Crucially, the anatomical and molecular details of sensing electric fields are still largely unknown in roots. A quantitative description of root electrotropism's kinetics is also missing, preventing a comparative analysis with animal electroreception and electrotaxis.

## Results

### *A novel root electrotropism assay*

To study for the first time root electrotropism in the plant model system *Arabidopsis thaliana,* we developed a new setup to stimulate, image and quantitate electrotropism in its primary root. Briefly, roots were grown vertically in a transparent chamber (V-box) containing a buffered liquid medium and two immersed electrodes connected to a power supply to generate a uniform electric field and an ionic current perpendicular to the growing roots (Fig. 1a and Methods).

To maintain a constant temperature and minimise the pH gradient generated by electrolysis, the liquid medium was continuously circulated in a closed loop between the V-box, a cooled water bath and a 2-litre reservoir bottle (Supplemental Fig. 1 and Methods). In each V-box, the primary roots of five seedlings were imaged every 10 minutes with a camera mounted in front of the V-box (Supplemental Fig. 1a and Methods). We measured the actual field generated in the medium by immersing voltmeter probes in the two neighbouring positions of each seedling: as expected, the field measured in the medium was lower than the nominal imposed in the air between the two electrodes, but still relatively uniform across the five positions (Supplemental Fig. 2a). At the same time, we measured the current passing through the circuit (Supplemental Fig. 2b and Methods).

To quantify the root response to the applied electric field, we took an image of the roots every 10 minutes and measured the angle between the root tip and the vertical gravity vector (Fig. 1b).

To confirm that the circulation of the liquid medium was effective in damping any pH gradient created by electrolysis and in eliminating any chemotropic effect, we imposed a field of 1.5 V/cm in a V-box without plants for one hour while maintaining liquid circulation. We then turned off the field and the liquid circulation, immediately positioned the plants in the V-box and imaged the roots for the next 80 minutes: we did not observe any significant deviation in root growth direction (t-test between 1.5 V/cm

and no field at 80 m, p=0.964), compared to roots in a V-box that never experienced the electric field (Supplemental Fig. 2c), indicating that no significant pH gradient was left in the medium.

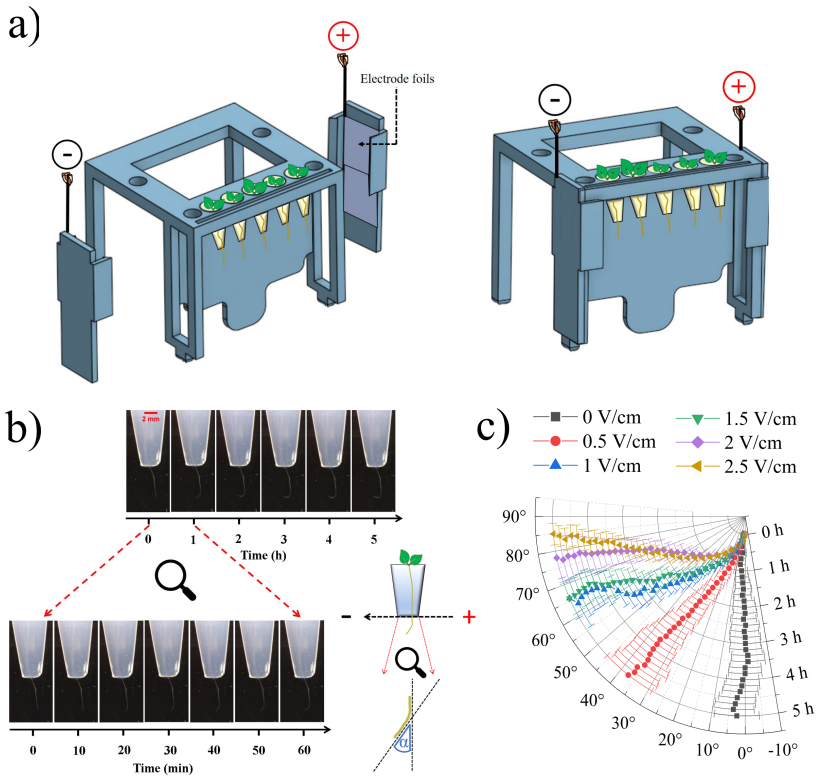


***Figure 1.*** **(a)** Schematic of the 3D-printed module used in the V-box. **(b)** Representative time-lapse series of a single root as imaged by the Raspberry camera from the V-box; inset, schematic of the angle measured. **(c)** Polar plot of the average root tip orientations relative to the to the gravity vector, with time on the radial axis and orientation angle on the circumferential axis; error bars, s.e.m.

*Root tip reorientation in an external electric field*

We measured the response of wild-type (WT) *Arabidopsis* primary roots to a continuous electric field. The distribution of reorientations to a range of fields intensities between 0.5 V/cm and 2.5 V/cm shows a quick tropism towards the negative electrode, or cathode (Fig. 1c).

We wondered how much of this effect was due to trivial electrostatic, *i.e.* the physical force perceived in the field by a hypothetical excess of positive charges on the root, as opposed to a more complex biological phenomenon. To address this, we pre-treated the roots in a 50 ℃ bath until growth and gravitropism were suppressed, transferred to the V-box and exposed them to a 2.0 V/cm electric field (Methods): the root response shows that this simple treatment was sufficient to completely inhibit electrotropism when compared to roots kept at a standard 23 ℃ temperature (t-test between 50 ℃ and 23 ℃ at 5 h, p<0.001), strongly suggesting that electrostatic alone could not explain the root response and that this is, in fact, a biological phenomenon (Supplemental Fig. 3).

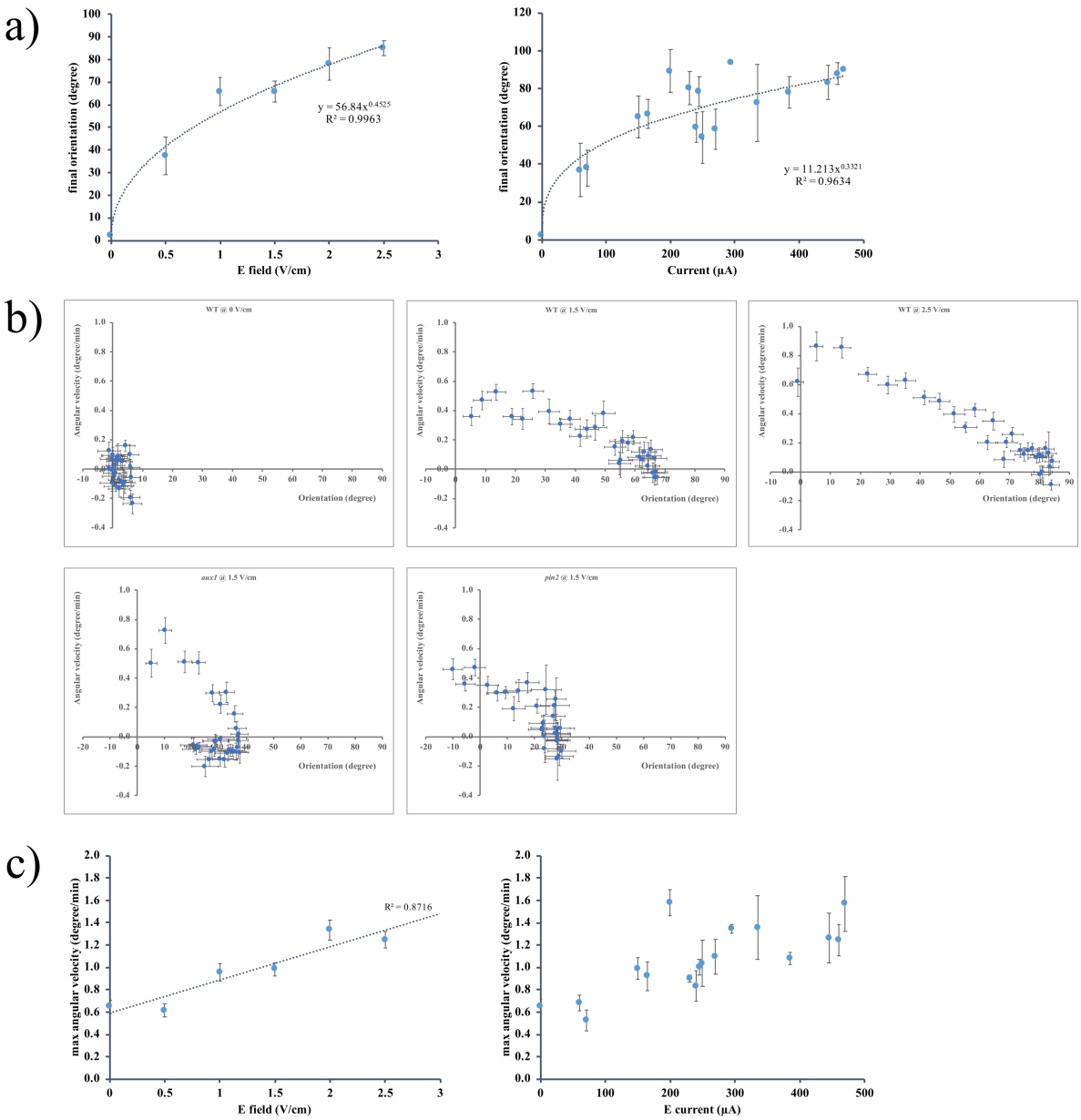


***Figure 2.*** **(a)** Root electrotropism response curves: average root tip orientations at 5hrs vs. electric field (left panel) or vs. current (right panel); error bars, s.e.m.; $R^2$, coefficient of determination. **(b)** Top row: WT root tip's average angular velocity at any observed orientation, for 0 V/cm (left panel), 1.5 V/cm (middle panel) and 2.5 V/cm (right panel); Bottom row: same plots for the mutants *aux1* (left panel) and *pin2* (right panel) at 1.5 V/cm; error bars, s.e.m. **(c)** Average maximum angular velocity reached by the root tip at a given electric field (left) or current (right); error bars, s.e.m.; $R^2$, coefficient of determination.

*Response curves*

The progressively sharper root tip reorientation as the field intensity was increased (Fig. 1c) suggests that the sensing mechanism is not acting as a simple on/off switch but that it can distinguish electric fields of different strengths. To quantitate this, we plotted the orientation angle at 5 h

("response") as a function of the electric field intensity ("stimulus"), and found the best fit with a power function with exponent 0.45 (Fig. 2a, left), indicating that the resolution of the sensor is higher at low-intensity stimuli (steep response curve) than at high-intensity stimuli (shallow response curve). The analogous response curve as a function of the measured current intensity is best fit with a power function with exponent 0.33 (Fig. 2a, right). Interestingly, power-law response curves with similar exponents have been traditionally measured in physiological responses to external stimuli in animal systems(Stevens, 1970): our results suggest that a power-law response to external stimuli might be a universal feature across life kingdoms and that it does not require a nervous system. Moreover, it might reveal constraints on the genetic architecture of the underlying sensory system(Adler et al., 2014).

Since the root tip reorientations did not show any obvious overshoot (Fig. 1c), we looked more closely at the angular velocity: the maximum average velocity in WT roots was reached when the root tip was between 10 and 20 degrees orientation to the gravity vector (Fig. 2b), and then progressively decreased as the root tip approached its maximum reorientation (Fig. 2b). This indicates that the mechanism can sense and respond differently to the changing relative orientation of the tip with the external electric field, and to progressively slow down the root tip rotation as it approaches the target orientation. Moreover, the maximum angular velocity appears to be roughly proportional to the electric field strength (Fig. 2c, left), although this is much less evident as a function of the electric current (Fig. 2c, right).

*Root tips are not damaged*

Early reports noted that protracted exposure to external fields could cause physical damage to plant root tips(Wawrecki and Zagórska-Marek, 2007). To control whether this was the case in our experimental conditions, we developed a simple chambered slide (V-slide) to be mounted on a standard confocal microscope stage (Supplemental Fig. 4a and Methods) with electrodes on the chamber's sides and a circulating liquid medium for temperature control similar to the one implemented in the V-box (Supplemental Fig. 4b). Seedlings from the *Arabidopsis* transgenic line constitutively expressing the yellow fluorescent cell-membrane marker WAVE131Y (Geldner et al., 2009) were mounted on the V-slide and imaged at cellular resolution while exposed to a 1.0 V/cm electric field (Methods). The field of view in our time-lapse images comprises the meristem, the transition zone and the distal elongation zone, but no cellular pattern perturbation was noticeable in any of these regions when compared to roots not exposed to the field (Supplemental Fig. 5).

Also, the same time-lapse suggests that asymmetric cell expansion in the elongation zone is causing the bending, as expected from other examples of root tropism (Gilroy, 2008).

*Regions of competence*

Since the root bending occurs in the elongation zone, we wanted to identify the region responsible for sensing the electric field. We excised distal fragments of the root at 125 μm, 300 μm, 400 μm and 500 μm from the tip (Fig. 3a), and then exposed the cut root to 1.5 V/cm (Methods).

In the first 2 h (Fig. 3b left), roots cut at 400 μm from the tip turned to angles indistinguishable from uncut roots exposed to the same field (Wilcoxon between 400 μm cut and uncut at 1.5 V/cm at 2 h, $p=0.211$), while roots cut at 500 μm from the tip did not turn and at 2 h showed orientations indistinguishable from uncut roots not exposed to a field (t-test between 500 μm cut at 1.5 V/cm and uncut at 0 V/cm at 2 h, $p=0.164$). These results indicate that the 400 μm distal fragment is not necessary for the early (2 h) electrotropic response, while the 500 μm distal fragment is; since the elongation zone involved in the bending spans an extended region proximal to the 500 μm cut, we

conclude that in *Arabidopsis* roots the region between 400 µm and 500 µm from the tip is necessary for early sensing an external electric field.

Between 2 h and 5 h of exposure (Fig. 3b right), while roots cut at 300µm on average continue to turn like the uncut roots (t-test between 300 µm cut and uncut at 1.5 V/cm at 5 hrs, p=0.071), roots cut at 400 µm quickly fail to sustain their response and at 5 h they show tip orientations on average different than those of uncut roots exposed to the same field (t-test between 400 µm cut and uncut at 1.5V/cm at 5 hrs, p<0.001). These results indicate that the 300 µm distal fragment is not necessary to maintain the electrotropic response up to 5hrs, while the 400 µm distal fragment is; we conclude that in *Arabidopsis* roots the region between 300 µm and 400 µm from the tip is necessary for prolonged sensing of the imposed electric field.

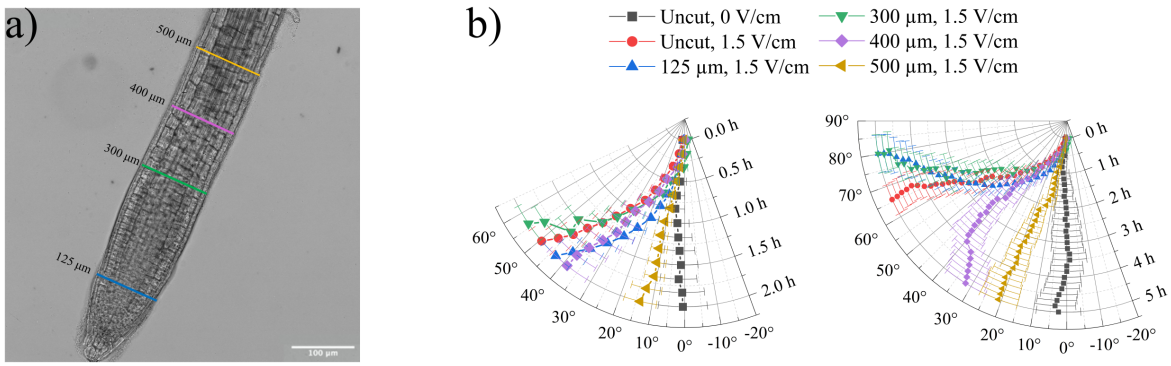


***Figure 3.*** **(a)** Points of excision overlapped to a microscope image of the *Arabidopsis* primary root tip; scale bar, 100 µm. **(b)** Polar plots of the average root tip orientations relative to the gravity vector, with time on the radial axis and orientation angle on the circumferential axis; the same data is presented for the first 2 h (left panel) and for the full 5 h (right panel); error bars, s.e.m.

*Auxin distribution is not altered by the electric field*

The fact that roots without tips could still respond to the electric field shows that even a major disruption of the stereotypical auxin redistribution mechanism is not sufficient to inhibit electrotropism.

On the other hand, an asymmetric accumulation of auxin is required for asymmetric cell elongation and root bending in some tropisms, as suggested by the classic Cholodny-Went model (Thimann and Went, 1937). To test whether this model applied to electrotropism and whether the external electric field is sufficient to induce an asymmetric distribution of auxin in the root, we exposed roots expressing the auxin-sensitive fluorescent reporter *R2D2* (Liao et al., 2015) to a field of 1.0 V/cm for 30 minutes, before quickly mounting them on a microscope slide and imaging them with a confocal microscope (Methods). A ratiometric quantification of *R2D2* signal in each epidermal cell (Fig. 4a; Supplemental Fig. 6 and Methods) showed that the average auxin response measured in the epidermal cells on the side facing the negative electrode and on the side facing the positive electrode were statistically indistinguishable (Fig. 4b; Methods), both in the distal (Wilcoxon test, p=0.696) and the proximal (Wilcoxon test, p=0.843) region of the root, indicating that auxin is not asymmetrically distributed after exposure to the electric field.

Moreover, both sides were also indistinguishable from the average between the two sides in roots not exposed to the field (mock), both in the distal (Wilcoxon test between the negative exposed side and mock, p=0.775; and between the positive exposed side and mock, p=0.881) and in the proximal

(Wilcoxon test between the negative exposed side and mock, p=0.041; and between the positive exposed side and mock, p=0.098) regions.

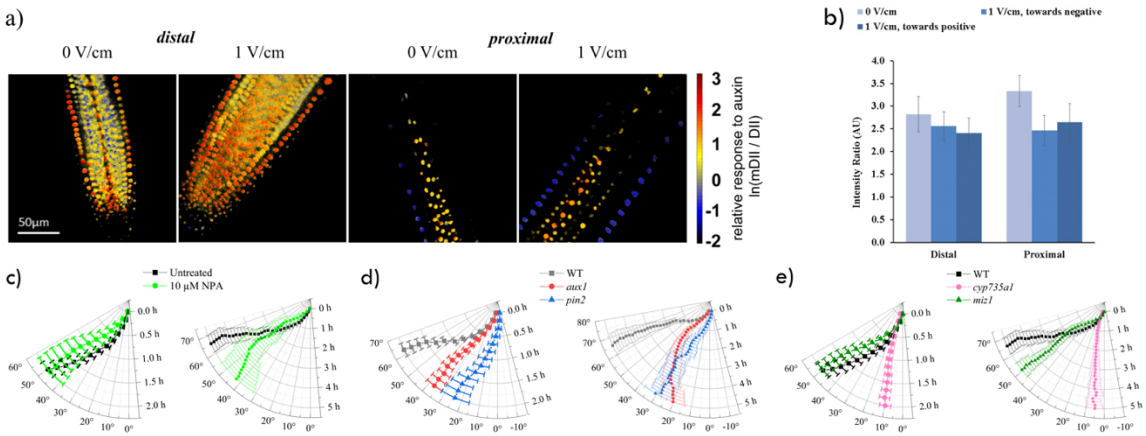


*Figure 4*. **(a)** Root tip images colour-coded to show the relative response to auxin concentration, as measured by the ratiometric fluorescent reporter R2D2 (see Methods); left panels: representative distal regions at 0 V/cm and 1 V/cm; right panels: representative proximal regions at 0 V/cm and 1 V/cm; scale bar, 50µm. **(b)** Quantification of the average relative response to auxin (as shown in a) in the epidermis cell layer facing the positive or negative electrode, in the distal and proximal regions; the data for 0 V/cm is an average between the two sides; error bars, s.e.m. (**c-e)** Polar plots of the average root tip orientations relative to the gravity, exposed to 1.5 V/cm, with time on the radial axis and orientation angle on the circumferential axis: NPA-treated (**c**), *aux1* and *pin2* (**d**), *cyp735a1* and *miz1* (**e**); error bars, s.e.m.

*Auxin transport is not necessary for early response*

Previous work indicated that auxin transport inhibitors can inhibit electrotropism response in maize roots(Ishikawa and Evans, 1990). To verify this in *Arabidopsis,* and further explore the role of auxin in root electrotropism, we used N-1-naphthylphthalamic acid (NPA) to inhibit polar auxin transport (Sabatini et al., 1999) while exposing the roots to the electric field. We tested 0.1 µM, 1.0 µM and 10 µM NPA and found that 10 µM NPA was the lowest concentration of NPA to inhibit gravitropism (Methods), a known auxin-dependent tropism.

We pre-treated the seedlings for 3 hours in liquid medium containing 10 µM NPA (Methods) and then transferred them to a V-box containing 10 µM NPA in the medium and the reservoir. In the first 2 hours of field exposure (Fig. 4c left) the NPA-treated roots reoriented at angles indistinguishable from those of untreated ones (Wilcoxon test between NPA-treated and mock at 2 h, p=0.684). From 2 to 5 hours of exposure (Fig. 4c right), NPA-treated roots seemed to return to a more vertical orientation compared to untreated roots, although not in a statistically significant way due to very large variance (t-test between NPA-treated and mock at 5 h, p=0.094). These results indicate that auxin polar transport is not necessary for an early electrotropic response, but might play a role in maintaining a long-term orientation.

To further explore the role of auxin transport, we tested the mutants of PIN2, an auxin cellular exporter(Chen et al., 1998), and mutants of AUX1, an auxin cellular importer (Marchant et al., 1999). Since *pin2* and *aux1* mutants do not respond to gravity, to obtain a sufficient number of roots growing vertically in preparation for the electrotropic assay, we wrapped the bottom part of the nursery boxes

with aluminium foil to induce negative root phototropism towards the bottom of the box (Methods). The same setup was used to germinate WT plants to be compared with these to mutants.

Roots of *pin2* mutants (Fig. 4d) showed a significant response (paired Wilcoxon between the time-points 0 h and 2 h, $p<0.01$; and between the time-points 0 h and 5 h, $p<0.01$), but weaker than WT (t-test between WT and *pin2* at 2 h, $p<0.01$; and between WT and *pin2* at 5 h, $p<0.01$) in the same conditions. Their angular velocity did not show an obvious decrease before reaching the target orientation, as with WT roots (Fig. 2b).

Analogously, roots of *aux1* mutants (Fig. 4d) showed a significant early response (paired t-test between the time-points 0 h and 2 h, $p<0.01$), but weaker than WT (t-test between WT and *pin2* at 2 h, $p<0.01$; t-test between WT and *pin2* at 5 h, $p<0.01$) in the same conditions. Interestingly, *aux1* roots on average failed to maintain their orientation for a longer period (paired t-test between the time-points 0 h and 5 h, $p=0.051$). Moreover, their angular velocity on average decreased while approaching the final orientation, as with WT roots (Fig. 2b).

Taken together, these results suggest that although auxin transport seems to play a role in maintaining a sustained response to the electric field, it is not necessary for triggering early electrotropism.

*Cytokinin biosynthesis is necessary for electrotropism*

Root hydrotropism, or the growth towards high concentration of water, was also previously shown to be largely independent of auxin distribution in *Arabidopsis* (Shkolnik et al., 2016), while it requires biosynthesis and asymmetric distribution of cytokinin (Chang et al., 2019), another plant hormone.

Given our results suggesting a limited role for auxin during electrotropism, we wondered if a cytokinin-dependent pathway similar to that involved in hydrotropism might play a role in electrotropism as well. We tested mutants of two genes required for the cytokinin-dependent hydrotropic response: *cyp735a1,* a cytochrome P450 monooxygenase enzyme necessary for the biosynthesis of the *trans*-zeatine variation of cytokinin (Takei et al., 2004) and for root hydrotropism (Chang et al., 2019), and *mizu-kussein1* (*miz1*), necessary for cytokinin asymmetric distribution in *Arabidopsis* roots (Chang et al., 2019) and for hydrotropism (Kobayashi et al., 2007).

Roots of *cyp735a1* mutants (Fig. 4e) failed to respond to the electric field, with tip orientations indistinguishable from that of WT roots not exposed to the field (t-test between *cyp735a1* exposed to 1.5 V/cm and WT not exposed at 5 h, $p=0.748$), showing that cytokinin biosynthesis is necessary for electrotropism in *Arabidopsis* roots.

Interestingly, roots of *miz1* mutants (Fig. 4e) showed an unperturbed electrotropic response in the first 2 h (Wilcoxon test between *miz1* and WT at 2 h, $p=0.859$) and perhaps a weakened response at 5 h, although not statistically significant (t-test between *miz1* and WT at 5 h, $p=0.033$), suggesting that the asymmetric distribution of cytokinin is not necessary for electrotropism.

Taken together, these surprising results indicate that cytokinin plays an important, although still unknown, role in root electrotropism.

## Discussion

The capability of plant roots to sense and combine numerous physical and chemical signals in the soil is quite extraordinary, notably in the absence of a centralised processing system. The more we understand about the physical and molecular mechanism behind the various root tropisms, the closer we will get to a complete understanding of signal integration in plants. In this work, we focused on the

little-studied phenomenon of root electrotropism and present its first quantitative characterisation in the flowering plant model system *Arabidopsis thaliana.*

A non-trivial observation from this work is that plant roots respond to weak (order of 1 V/cm and 100 μA) external electric fields and currents in a progressive way, with an increasingly stronger tendency to align with the field as the field and current intensities increase. This is interesting because it reveals a sophisticated way to discriminate between highly charged particles (*e.g.* ions, micro-organisms, other plant roots) and weakly charged ones. At the same time, the absence of overshooting also points to a mechanism that perhaps can be modelled along the lines of a proportional–integral–derivative control system (Chevalier et al., 2019). Moreover, we show that the kinetics (response curve) of root electrotropism follows a power-law reminiscent of the Stevens law used to describe physiological responses in animal biosensors (Stevens, 1970), which could shed some light on the underlying genetic network (Adler et al., 2014) and at the same time suggest the existence of universal classes of biosensing mechanisms spanning across biological kingdoms.

An unexpected result from this work is that the root cap is not necessary for electrotropism. This comes from our root tip excision experiments and is in contrast to other root tropisms where the cap is in fact required for sensing: gravitropism (Juniper et al., 1966), thigmotropism (Massa and Gilroy, 2003) and phototropism (Mullen et al., 2002). Interesting, other regions besides the root cap has also be involved in gravitropism (Wolverton et al., 2002), while hydrotropism does not require the 250μm distal region in the *Arabidopsis* root (Dietrich et al., 2017).

Moreover, we identified two proximal regions required for the detection of the field: the segment between roughly 400 μm and 500 μm from the tip is necessary for the early detection (within 2 h from exposure), while the segment between roughly 300 μm and 400 μm is necessary for a prolonged detection (up to 5 h from exposure). Interestingly, these regions seem to correspond to the anatomically well-characterised transition zone, between the meristem and the elongation zone, which has been previously involved in root sensing (Baluška et al., 2010; Muthert et al., 2020). In future works, it will be crucial to discern whether electrotropism sensing relies on a broad region like the transition zone or if it can be narrowed down to a more specific cell population therein.

Taken together, the results above suggest that environmental sensing in the root are distributed across more than one cell type and that signal integration would require non-cell-autonomous molecular and/or physical mechanisms.

Interestingly, previous studies suggested that the movement of Ca++ ions accumulated in the mucilage at the very tip of the root might be involved in the electrotropic sensing (Marcum and Moore, 1990). Since any excision above 125 μm from the tip essentially removes all the mucilage from the root, our data do not support this hypothesis for *Arabidopsis*.

Finally, our results suggest that auxin asymmetric distribution is not required for electrotropism in *Arabidopsis*, similarly to what found for hydrotropism (Shkolnik et al., 2016) and phototropism (Kimura et al., 2018). Instead, the data suggest that cytokinin plays a role, although future studies will have to investigate its role even further.

## Materials and Methods

*Plant material*

Wild-type and mutant *Arabidopsis thaliana* plants were all from the Columbia (Col-0) ecotype; the following mutant alleles were used: *aux1-7* (NASC id 9583) for *aux1*, *eir1-1* (NASC id 8058) for *pin2, miz1-2* for *miz1* (NASC id N576560) and *cyp735a1* (NASC id N593028). The fluorescent line

322 *WAVE131Y* is expressing *pUBQ10::WAVE131:YFP* (NASC id N781535); the fluorescent line *R2D2*
323 is expressing *RPS5A-mDII-ntdTomato, RPS5A-DII-n3xVenus* (courtesy of Dr Teva Vernoux).
324 Seeds were imbibed in water and kept in the dark for 2 days at 4 °C to synchronise germination. All
325 seeds were surface sterilised using 50% v/v Haychlor bleach and 0.0005% v/v Triton X-100 for 3
326 minutes and then rinsed 6 times with sterilised milliQ water. Seed germination protocols are described
327 in the experiment-specific Methods sections below. All experiments were conducted on with primary
328 roots of seedlings 5-8 days post-germination.
329
330 *Electrotropism assay (V-box)*
331 Seeds were sown individually inside PCR tubes filled with 1X MS gel medium: 0.44% w/v Murashige
332 and Skoog (MS) Basal medium (Sigma-Aldrich, M5519), 0.5% w/v sucrose, 0.05% w/v MES hydrate
333 (Sigma-Aldrich M8250), 0.8% w/v agar (Sigma-Aldrich 05040), pH adjusted to 5.7 with TRIS HCl
334 (Fisher-Scientific 10205100). The PCR tubes had their end cut out to allow the root to grow through
335 and placed in a 3D-printed (Ultimaker 2+) holder inserted in a Magenta box (Sigma-Aldrich V8380).
336 The Magenta box was filled with 150 ml of 1/500X MS liquid medium (0.00088% w/v MS Basal
337 medium, 0.5% w/v sucrose, 0.05% w/v MES hydrate, pH5 adjusted to 5.7 with TRIS HCl) to reach
338 the end of the PCR tubes. These "germination" or "nursery" boxes were placed in a growth chamber
339 at 23 °C, with a 16 h/8 h light/dark photoperiod and light intensity 120 μmol/m$^2$s.
340 In preparation for the electrotropism assay, each PCR tube containing a single 7 to 10-day-old
341 seedling was transferred to a modified 3D-printed holder in a Magenta box filled with 1/500X MS liquid
342 medium. The modified module consisted of a main body with five holes for the PCR tubes containing
343 the seedlings, and two side clips to position the electrodes consisting of platinum-iridium
344 (Platinum:Iridium = 80:20; Alfa Aesar 41805.FF) foils (Fig. 1a), which were connected to an external
345 power supply. In this paper, we refer to the Magenta box and its holder as the "V-box". In addition to
346 the five holes for the plants, four extra holes were designed on the stand: two at each end of the front
347 side to pump the medium out of the V-box, and two more on the back to pump the medium in, using
348 a tubing system and peristaltic pumps (Verdeflex AU R2550030 RS1) to circulate the medium at a
349 speed of 1 ml/sec to and from a 2 l reservoir bottle (Supplemental Fig. 1). Crucially, between the V-
350 box and the reservoir bottle, the tubings were immersed in a cooled water bath (Grant Instruments,
351 LTDGG) maintained at the constant temperature of 19 ℃ (Supplemental Fig. 1), which was enough
352 to maintain the medium inside the v-box at a constant 23 ℃, as measured. All electrotropic
353 experiments were performed at constant illumination.
354 The electric field was generated with a power supply attached to the platinum-iridium foil electrodes
355 that were immersed in the liquid medium in the V-box. Standard electric wires were soldered on the
356 top of two electrodes, always kept outside the liquid medium to avoid contaminants from the solder.
357 The voltage was set constant on the power supply, while the current was measured independently
358 with a multimeter in series.
359 To record the movement of the roots over time, a Raspberry Pi camera module V2 (913-2664)
360 connected to a Raspberry Pi board module B+ (137-3331) was used. The Raspberry Pi was
361 programmed to take a picture every 10 minutes, using the command *crontab* in the local Raspbian
362 OS.
363 WT electrotropism assays were performed with the following sample sizes: 0 V/cm, N=10; 0.5 V/cm,
364 N=9; 1.0 V/cm, N=8; 1.5 V/cm, N=21; 2.0 V/cm, N=18; 2.5 V/cm, N=20.
365 Mutants electrotropism assays were performed with the following sample sizes: *aux1*, N=18; *pin2*,
366 N=13; *cyp735a1*, N=20; *miz1*, N=9.
367 The control for medium circulation efficiency was performed with the following sample sizes: 1.5
368 V/cm, N=5; 0 V/cm, N=10.

369
370 *High-temperature treatment*
371 Wild-type Col-0 seeds were germinated and grown for 7 to 10 days in the nursery boxes as
372 described in the Electrotropism Assay section. The boxes undergoing treatment were then immersed
373 in a water bath set at 45 °C or 50 °C, for 10 minutes. The PCR tubes containing the seedlings were
374 then transferred to a V-box, exposed to an electric field of 2.0 V/cm for 5 hours and imaged, as
375 described in the Electrotropism Assay section.
376 Electrotropism assays for excised roots were performed with the following sample sizes: 23℃,
377 N=18; 45℃, N=5; 50℃, N=5.
378 For the gravitropism control, seedlings were treated with high temperature as described above and
379 then transferred on 1X MS agar plates, to complete the assay as described in the Gravitropic Assay
380 section.
381
382 *Electrotropism on a microscope (V-slide)*
383 Seeds of the transgenic reporter line *WAVE131Y* (see Plant Material section) were germinated on
384 1X MS agar medium (0.44% w/v MS Basal medium, 0.5% w/v sucrose, 0.05% w/v MES hydrate, pH
385 adjusted to 5.7 with TRIS HCl, 0.8% w/v agar) in square plates kept vertical in a growth chamber at
386 22 °C, with a 16 h/8 h light/dark photoperiod.
387 At 2 days post-germination the seedlings were mounted on the V-slide with 1/500X MS liquid
388 medium (0.00088% w/v MS Basal medium, 0.5% w/v sucrose, 0.05% w/v MES hydrate, pH5 adjusted
389 to 5.7 with TRIS HCl). The V-slide was then connected to the medium perfusion system circulating
390 the same 1/500X MS medium, and the V-slide's electrodes were connected to the power supply
391 (Voltcraft PS-1302-D).
392 Imaging was performed on a Leica SP5 laser scanning confocal microscope with 20X air objective,
393 while the liquid medium was circulated, and the electric field maintained constant. Fluorophore was
394 excited with the 514 nm Argon laser line and the emission collected with PMT detector at 524-570
395 nm. Images were collected at intervals of 2 minutes.
396
397 *Root tip excisions*
398 Seeds were germinated in nursery boxes as described.
399 At 3 days post-germination, seedlings were transferred to hard 1X MS agar medium (0.44% w/v MS
400 Basal medium, 0.5% w/v sucrose, 0.05% w/v MES hydrate, pH adjusted to 5.7 with TRIS HCl, 5.0%
401 agar) and manually dissected using a dental needle (Sterican, 27G) under a dissecting microscope
402 (Nikon SMZ1000) at 180X magnification, following the published protocol (Kral et al., 2016).
403 After root tip excision, the seedlings were immediately moved into the V-box for the electrotropism
404 assay.
405 Electrotropism assays on excised roots were performed with the following sample sizes: 125 µm,
406 N=16; 300 µm, N=7; 400 µm, N=10; 500 µm, N=10; uncut at 0 V/cm, N=10; uncut at 1.5 V/cm, N=21.
407
408 *R2D2 reporter*
409 Seeds of the transgenic reporter line *R2D2* (see Plant Material section) were germinated in nursery
410 boxes and exposed to 1.0 V/cm for 30min in V-boxes, as described in the Electrotropism Assay
411 section. After exposure, *R2D2* roots were quickly mounted on standard microscope slides with sterile
412 deionised water and imaged using Leica SP5 laser scanning confocal microscope, with 63X water
413 immersion objective.
414 *R2D2* expresses two versions of a protein that forms a complex with auxin: DII-n3xVENUS, which
415 is degraded within minutes upon binding with auxin; mDII-ntdTOMATO, which contains a modified,

416 non-degradable, version of DII. Both of the proteins are localised in the nucleus. We followed the
417 published protocol (Liao et al., 2015) to separately collect the emission from mDII-ntdTOMATO
418 (Supplemental Fig. 6a) and DII-n3xVENUS (Supplemental Fig. 6b).
419 For each root, a mean background was defined as the average pixel intensity in the mDII channel
420 of an 80x80 pixels corner of the field of view not occupied by the root. The mean background was
421 then subtracted from all pixel intensities in both channels (mDII and DII). We manually segmented
422 with FIJI (Schindelin et al., 2012) the most visible cell nuclei in the epidermis of each root, both in the
423 distal (12 roots in mock conditions and 16 roots exposed to the field) and in the proximal (11 roots in
424 mock conditions and 13 roots exposed to the field) regions of the root tip, and quantified the average
425 pixel intensity (corrected after background subtraction) for each segmented nucleus. Finally, we
426 calculated the natural log of the ratio between the average mDII (non-degradable, auxin-independent)
427 and DII (degradable, auxin-dependent) signals in each nucleus and mapped it on top of the root
428 image (Supplemental Fig. 6d).
429 For each root, we calculated the average and standard deviation of these ratios, for epidermal nuclei
430 facing the anode or the cathode (Fig. 4b).
431 Sample size as following: exposed to E field and imaged in the distal region, N=16; exposed to E
432 field and imaged in the proximal region, N=13; not exposed to E field and imaged in the distal region,
433 N=24; not exposed to E field and imaged in the proximal region, N=22.
434
435 *NPA treatment*
436 To find the minimum concentration of N-1-naphthylphthalamic acid (NPA) that inhibits gravitropism,
437 seeds were germinated on 1X MS agar medium (0.44% w/v MS Basal medium, 0.5% w/v sucrose,
438 0.05% w/v MES hydrate, pH adjusted to 5.7 with TRIS HCl, 0.8% w/v agar) and at 3 days post-
439 germination were transferred for 3 hrs into cell culture dishes containing 5 ml of 1/500X MS liquid
440 medium (0.00088% w/v MS Basal medium, 0.5% w/v sucrose, 0.05% w/v MES hydrate, pH5 adjusted
441 to 5.7 with TRIS HCl) plus NPA at 0.1 μM, 1.0 μM and 10 μM. The seedlings were then transferred
442 onto 1/500X MS agar plates (0.00088% w/v MS Basal medium, 0.5% w/v sucrose, 0.05% w/v MES
443 hydrate, pH5 adjusted to 5.7 with TRIS HCl, 0.8% w/v agar) containing the same concentration of
444 NPA. The plates were moved to a growth room (22 °C, 16 h/8 h light/dark photoperiod), rotated by
445 90 degrees and monitored for root gravitropic response.
446 To quantify the effect of NPA on electrotropism, after being treated with a concentration of 10 μM
447 NPA for 3 hours as described above, the seedlings were transferred inside a V-box and exposed to
448 a 1.5 V/cm electric field as described in the Electrotropism Assay section. Both the V-box and the
449 reservoir bottle contained 10 μM NPA throughout the experiment.
450 Samples sizes were the following: mock-treated, N=21; 10 μM NPA treated, N=8.
451
452 *Gravitropism assay*
453 Seeds were germinated on 1X MS agar medium (0.44% w/v MS Basal medium, 0.5% w/v sucrose,
454 0.05% w/v MES hydrate, pH adjusted to 5.7 with TRIS HCl, 0.8% w/v agar) in square plates kept
455 vertical in a growth chamber at 22°C, with a 16 h/8 h light/dark photoperiod and light intensity 120
456 μmol/ $m^2$s.
457 At 3 days post-germination the plates were rotated by 90 degrees, and the root tips monitored for
458 gravitropic response in the following 24 h.
459
460 *Statistical analysis*
461 When comparing two samples of measurements, each distribution was first checked for normality
462 with the Shapiro-Wilk test with alpha-level = 0.05. Normal distributions were tested with the two-tails

Student's t-test without assuming equal variances (Welch two-sample t-test); if one of the two distributions were not normal, the non-parametric Mann-Whitney U (Wilcoxon) test was used. Unless stated otherwise, all comparisons were performed assuming independence (unpaired test). All statistical tests were performed with R.

**Acknowledgements**

We thank T. Vernoux for providing seeds of the *R2D2* line; A. Guyon, O. Kranse, C. Keyzor, C.D. Livesey-Clare for generous technical help; M. Levin and I. Bordeu for critical discussions at various stages of the project. This work was partly supported by the BBSRC Impact Acceleration Account BB/S506667/1 and the Allen Discovery Center at Tufts University; N.K. was supported by the BBSRC DTP grant BB/M011178/1.

**Competing Interest Statement:** The authors declare no competing interests.

## References

Adler M, Mayo A, Alon U. 2014. Logarithmic and Power Law Input-Output Relations in Sensory Systems with Fold-Change Detection. *Plos Comput Biol* **10**:e1003781. doi:10.1371/journal.pcbi.1003781

Baluška F, Mancuso S, Volkmann D, Barlow PW. 2010. Root apex transition zone: a signalling–response nexus in the root. *Trends in Plant Science* **15**:402–408. doi:10.1016/j.tplants.2010.04.007

Chang J, Li X, Fu W, Wang J, Yong Y, Shi H, Ding Z, Kui H, Gou X, He K, Li J. 2019. Asymmetric distribution of cytokinins determines root hydrotropism in Arabidopsis thaliana. *Cell Res* **29**:984–993. doi:10.1038/s41422-019-0239-3

Chen R, Hilson P, Sedbrook J, Rosen E, Caspar T, Masson PH. 1998. The Arabidopsis thaliana AGRAVITROPIC 1 gene encodes a component of the polar-auxin-transport efflux carrier. *Proc National Acad Sci* **95**:15112–15117. doi:10.1073/pnas.95.25.15112

Chevalier M, Gómez-Schiavon M, Ng AH, El-Samad H. 2019. Design and Analysis of a Proportional-Integral-Derivative Controller with Biological Molecules. *Cell Syst* **9**:338-353.e10. doi:10.1016/j.cels.2019.08.010

Clarke D, Whitney H, Sutton G, Robert D. 2013. Detection and learning of floral electric fields by bumblebees. *Science* **340**:66–69. doi:10.1126/science.1230883

Crampton WGR. 2019. Electroreception, electrogenesis and electric signal evolution. *J Fish Biol* **95**:92–134. doi:10.1111/jfb.13922

Dietrich D, Pang L, Kobayashi A, Fozard JA, Boudolf V, Bhosale R, Antoni R, Nguyen T, Hiratsuka S, Fujii N, Miyazawa Y, Bae T-W, Wells DM, Owen MR, Band LR, Dyson RJ, Jensen OE, King JR, Tracy SR, Sturrock CJ, Mooney SJ, Roberts JA, Bhalerao RP, Dinneny JR, Rodriguez PL, Nagatani A, Hosokawa

Y, Baskin TI, Pridmore TP, Veylder LD, Takahashi H, Bennett MJ. 2017. Root hydrotropism is controlled via a cortex-specific growth mechanism. *Nature Plants* **3**:17057. doi:10.1038/nplants.2017.57

Elfving F. 1882. Ueber eine Wirkung des galvanischen Stromes auf wachsende Wurzeln. *Bot Zeit* 257–264.

Ewart AJ, Bayliss JS. 1905. On the nature of the galvanotropic irritability of roots. *Proc Royal Soc Lond Ser B Contain Pap Biological Character* **77**:63–66. doi:10.1098/rspb.1905.0058

Geldner N, Dénervaud-Tendon V, Hyman DL, Mayer U, Stierhof Y-D, Chory J. 2009. Rapid, combinatorial analysis of membrane compartments in intact plants with a multicolor marker set. *The Plant journal : for cell and molecular biology* **59**:169–178. doi:10.1111/j.1365-313x.2009.03851.x

Gilroy S. 2008. Plant tropisms. *Current Biology* **18**:R275-7. doi:10.1016/j.cub.2008.02.033

Iino M. 2006. Toward understanding the ecological functions of tropisms: interactions among and effects of light on tropisms. *Curr Opin Plant Biol* **9**:89–93. doi:10.1016/j.pbi.2005.11.012

Ishikawa H, Evans ML. 1990. Electrotropism of maize roots. Role of the root cap and relationship to gravitropism. *Plant physiology* **94**:913–918.

Juniper BE, Groves S, Landau-Schachar B, Audus LJ. 1966. Root Cap and the Perception of Gravity. *Nature* **209**:93–94. doi:10.1038/209093a0

Kimura T, Haga K, Shimizu-Mitao Y, Takebayashi Y, Kasahara H, Hayashi K-I, Kakimoto T, Sakai T. 2018. Asymmetric Auxin Distribution is Not Required to Establish Root Phototropism in Arabidopsis. *Plant Cell Physiology* **59**:828–840. doi:10.1093/pcp/pcy018

Kobayashi A, Takahashi A, Kakimoto Y, Miyazawa Y, Fujii N, Higashitani A, Takahashi H. 2007. A gene essential for hydrotropism in roots. *Proc Natl Acad Sci U S A* **104**:4724–4729. doi:10.1073/pnas.0609929104

Kral N, Ougolnikova AH, Sena G. 2016. Externally imposed electric field enhances plant root tip regeneration. *Regeneration (Oxford, England)* **3**:156–167. doi:10.1002/reg2.59

Kutschera U, Briggs WR. 2012. Root phototropism: from dogma to the mechanism of blue light perception. *Planta* **235**:443–452. doi:10.1007/s00425-012-1597-y

Liao C-Y, Smet W, Brunoud G, Yoshida S, Vernoux T, Weijers D. 2015. Reporters for sensitive and quantitative measurement of auxin response. *Nature methods* **12**:207–210. doi:10.1038/nmeth.3279

Marchant A, Kargul J, May ST, Muller P, Delbarre A, Perrot-Rechenmann C, Bennett MJ. 1999. AUX1 regulates root gravitropism in Arabidopsis by facilitating auxin uptake within root apical tissues. *Embo J* **18**:2066–2073. doi:10.1093/emboj/18.8.2066

Marcum H, Moore R. 1990. Influence of Electrical Fields and Asymmetric Application of Mucilage on Curvature of Primary Roots of Zea mays. *American Journal of Botany* **77**:446. doi:10.2307/2444378

Massa GD, Gilroy S. 2003. Touch modulates gravity sensing to regulate the growth of primary roots of Arabidopsis thaliana. *The Plant Journal* **33**:435–445. doi:10.1046/j.1365-313x.2003.01637.x

McGillivray AM, Gow NAR. 1986. Applied Electrical Fields Polarize the Growth of Mycelial Fungi. *Microbiology* **132**:2515–2525. doi:10.1099/00221287-132-9-2515

Miyazawa Y, Takahashi H. 2019. Molecular mechanisms mediating root hydrotropism: what we have observed since the rediscovery of hydrotropism. *J Plant Res* **133**:3–14. doi:10.1007/s10265-019-01153-3

Mullen JL, Wolverton C, Ishikawa H, Hangarter RP, Evans ML. 2002. Spatial separation of light perception and growth response in maize root phototropism. *Plant Cell Environ* **25**:1191–1196. doi:10.1046/j.1365-3040.2002.00899.x

Muthert LWF, Izzo LG, Zanten M van, Aronne G. 2020. Root Tropisms: Investigations on Earth and in Space to Unravel Plant Growth Direction. *Front Plant Sci* **10**:1807. doi:10.3389/fpls.2019.01807

Navez AE. 1927. Galvanotropism of roots. *The Journal of general physiology* **10**:551–558.

Peters RC, Eeuwes LBM, Bretschneider F. 2007. On the electrodetection threshold of aquatic vertebrates with ampullary or mucous gland electroreceptor organs. *Biol Rev* **82**:361–373. doi:10.1111/j.1469-185x.2007.00015.x

Sabatini S, Beis D, Wolkenfelt H, Murfett J, Guilfoyle T, Malamy J, Benfey P, Leyser O, Bechtold N, Weisbeek P, Scheres B. 1999. An auxin-dependent distal organizer of pattern and polarity in the Arabidopsis root. *Cell* **99**:463–472. doi:10.1016/s0092-8674(00)81535-4

Schindelin J, Arganda-Carreras I, Frise E, Kaynig V, Longair M, Pietzsch T, Preibisch S, Rueden C, Saalfeld S, Schmid B, Tinevez J-Y, White DJ, Hartenstein V, Eliceiri K, Tomancak P, Cardona A. 2012. Fiji: an open-source platform for biological-image analysis. *Nature methods* **9**:676–682. doi:10.1038/nmeth.2019

Shanley LJ, Walczysko P, Bain M, MacEwan DJ, Zhao M. 2006. Influx of extracellular Ca2+ is necessary for electrotaxis in Dictyostelium. *J Cell Sci* **119**:4741–4748. doi:10.1242/jcs.03248

Shkolnik D, Krieger G, Nuriel R, Fromm H. 2016. Hydrotropism: Root Bending Does Not Require Auxin Redistribution. *Mol Plant* **9**:757–759. doi:10.1016/j.molp.2016.02.001

Stenz HG, Weisenseel MH. 1993. Electrotropism of Maize (Zea-Mays L) Roots - Facts and Artifacts. *Plant physiology* **101**:1107–1111. doi:10.1104/pp.101.3.1107

Stevens SS. 1970. Neural Events and the Psychophysical Law: Power functions like those that govern subjective magnitude show themselves in neurelectric effects. *Science* **170**:1043–1050. doi:10.1126/science.170.3962.1043

Su S-H, Gibbs NM, Jancewicz AL, Masson PH. 2017. Molecular Mechanisms of Root Gravitropism. *Current Biology* **27**:R964–R972. doi:10.1016/j.cub.2017.07.015

Sukul NC, Croll NA. 1978. Influence of potential difference and current on the electrotaxis of Caenorhaditis elegans. *J Nematol* **10**:314–7.

Sutton GP, Clarke D, Morley EL, Robert D. 2016. Mechanosensory hairs in bumblebees (Bombus terrestris) detect weak electric fields. *Proceedings of the National Academy of Sciences* **113**:7261–7265. doi:10.1073/pnas.1601624113

Takei K, Yamaya T, Sakakibara H. 2004. Arabidopsis CYP735A1 and CYP735A2 Encode Cytokinin Hydroxylases That Catalyze the Biosynthesis of trans-Zeatin. *J Biol Chem* **279**:41866–41872. doi:10.1074/jbc.m406337200

Thimann KV, Went FW. 1937. Phytohormones. doi:10.5962/bhl.title.5695

Wawrecki W, Zagórska-Marek B. 2007. Influence of a Weak DC Electric Field on Root Meristem Architecture. *Ann Bot-london* **100**:791–796. doi:10.1093/aob/mcm164

Wolverton C, Mullen JL, Ishikawa H, Evans ML. 2002. Root gravitropism in response to a signal originating outside of the cap. *Planta* **215**:153–157. doi:10.1007/s00425-001-0726-9

Wolverton C, Mullen JL, Ishikawam H, Evans ML. 2000. Two distinct regions of response drive differential growth in Vigna root electrotropism. *Plant Cell Environ* **23**:1275–1280. doi:10.1046/j.1365-3040.2000.00629.x

**Supplemental Figure 1**

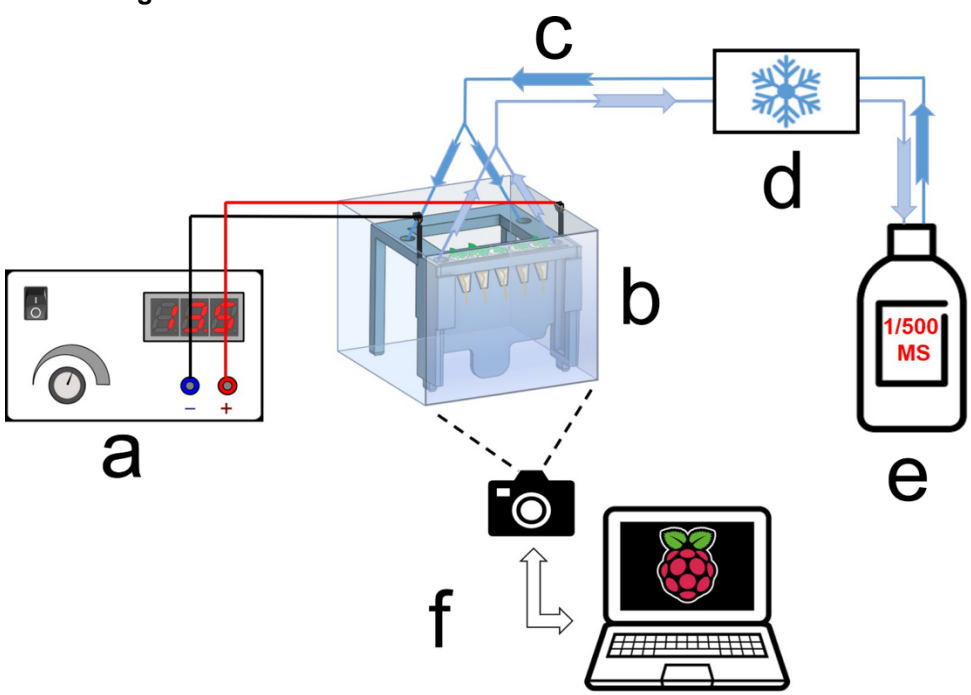


Diagram of the complete setup used for the electrotropism assay. **(a)** Power supply connected to the electrodes in the V-box. **(b)** V-box. **(c)** Flexible tubing bringing liquid medium in and out the V-box. **(d)** Chilled water bath. **(e)** Medium reservoir. **(f)** RaspberryPi camera

**Supplemental Figure 2**

a)

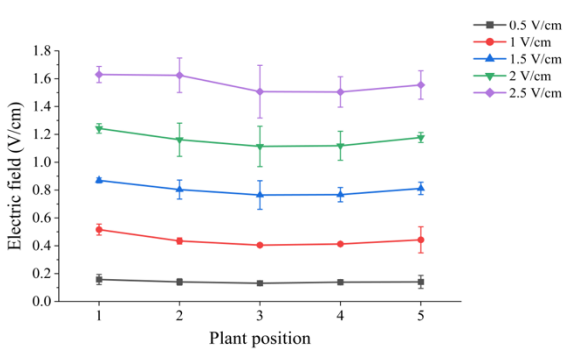


b)

| Electric field (V/cm) | Current (µA) |
|---|---|
| 0.5 | 65.5 ± 5.8 |
| 1 | 157.5 ± 7.9 |
| 1.5 | 247.7 ± 13.3 |
| 2 | 264.7 ± 78.8 |
| 2.5 | 438.5 ± 40.8 |

c)

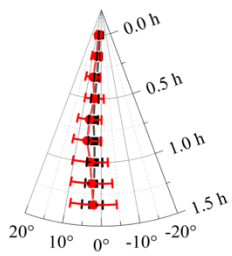


V-box characterization. **(a)** Average electric field measurements inside the V-box at each of the five plant positions (N=3 measurements), for each voltage difference imposed by the power supply between the electrodes; error bars, s.e.m. (**b)** Average (+/- standard deviation) electric currents measured in the circuit for each voltage difference imposed by the power supply between the electrodes. **(c)** Control for efficient circulation of the liquid medium: polar plot of the average root tip orientations relative to the gravity vector, with time on the radial axis and orientation angle on the circumferential axis, of unexposed roots inside a V-box that had been pre-exposed to 1.5 V/cm or 0 V/cm; error bars, s.e.m.

**Supplemental Figure 3**

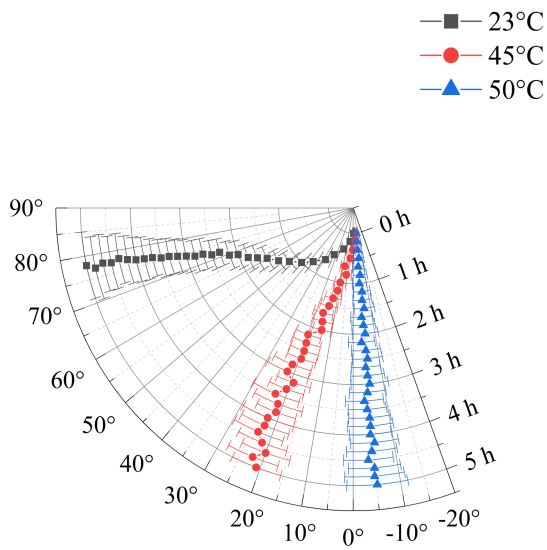


Live *vs* dead root. Polar plot of the average root tip orientations relative to the gravity vector, with time on the radial axis and orientation angle on the circumferential axis, for roots pre-treated to 23 ℃, 45 ℃ or 50 ℃ and then exposed to 2.0 V/cm; error bars, s.e.m.

**Supplemental Figure 4**

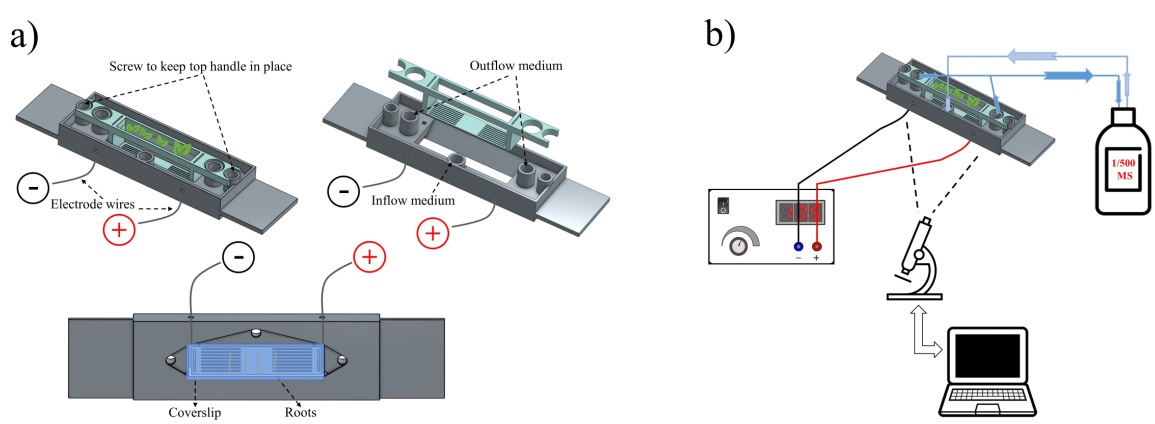


V-slide. **(a)** Diagram of the V-slide used to image with confocal microscopy a root exposed to the electric field. **(b)** Diagram of the complete setup used with the V-slide.

**Supplemental Figure 5**

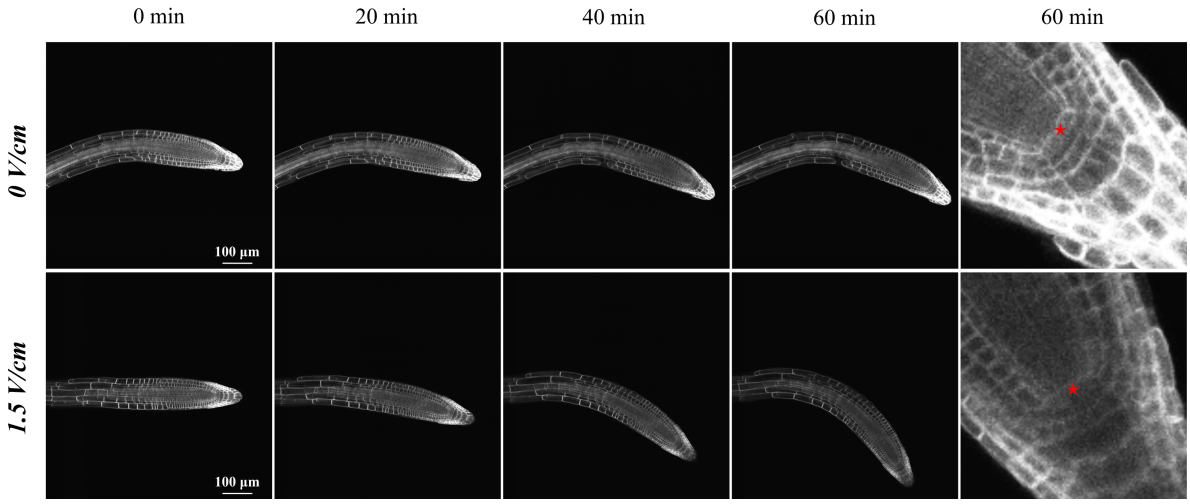


Root meristem is not damaged. Time-lapse confocal images of two representative roots (total roots observed: N=3 for mock and N=3 for 1.5 V/cm) expressing the WAVE131Y marker, exposed to 0 V/cm or 1.5 V/cm in the V-slide; red star, the quiescent centre (QC); scale bars, 100 µm.

**Supplemental Figure 6**

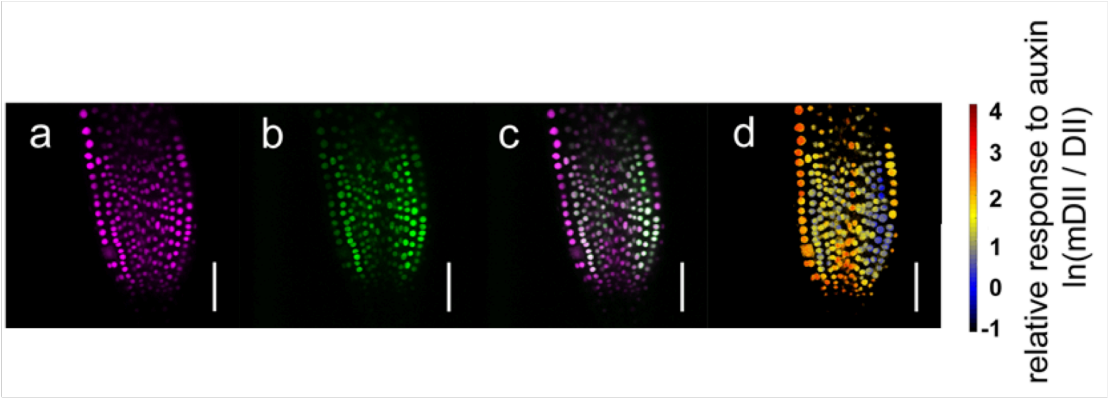


R2D2 ratiometric image. **(a)** Signal collected from the non-degradable mDII::ntdTomato. (**b)** Signal collected from the degradable DII:n3xVenus. **(c)** Overlay image of the two channels. **(d)** Ratio image of the two channels, higher ratio indicates higher auxin. Values for the colours used in the ratio image are shown next to the colour bar, standing for the relative response to auxin $\ln\frac{\mathrm{mDII}}{\mathrm{DII}}$ . Scale bars, 50µm.